BAU Journal - Science and Technology

Volume 3 | Issue 1
ISSN: 2706-784X

Article 4

December 2021

THE INHIBITION ACTIVITY OF TERT-BUTYLHYDROQUINONE TOWARDS CORROSION OF ALUMINUM, COPPER AND STAINLESS STEEL IN BIODIESEL BLEND B20 ALTERNATIVE FUEL

Chaza Joumaa
Post Graduate Student, Faculty of Science, Beirut Arab University, Lebanon, chj349@student.bau.edu.lb

Ibtissam Saad
Doctor, Faculty of Science, Beirut Arab University, Lebanon, ibtissam.saad@bau.edu.lb

Ghassan Younes
Head of Chemistry Department and Professor of Physical Chemistry, Faculty of Science, Beirut Arab University, Lebanon, ghass@bau.edu.lb

THE INHIBITION ACTIVITY OF TERT-BUTYLHYDROQUINONE TOWARDS CORROSION OF ALUMINUM, COPPER AND STAINLESS STEEL IN BIODIESEL BLEND B20 ALTERNATIVE FUEL

Abstract

Tert-butylhydroquinone (TBHQ) has been investigated as corrosion inhibitor for aluminum; copper and stainless steel in biodiesel blend B20 by using electrochemical impedance spectroscopy (EIS) method. The results showed that the inhibition efficiency increases with an increase in the concentration of TBHQ but decreases with increasing temperature from 30°C to 60°C. A maximum inhibition efficiency of about 61.52% for aluminum was recorded for THBQ in biodiesel blend B20 at temperature 30°C and at a concentration of $4x10^{-6}$ M which is the lowest concentration used compared to the concentrations of TBHQ used for the other metals (copper and stainless steel). Theoretical fitting of different isotherms, namely Langmuir, Freundlich, Kinetic-Thermodynamic and Flory-Huggins models were tested to clarify the nature of TBHQ adsorption on the three metal surfaces. The obtained experimental data best fitted Freundlich and Kinetic-Thermodynamic. In addition, the thermodynamic parameters of corrosion and adsorption processes were calculated and discussed. The sign of the Gibb's free energy of the adsorption obtained suggested that inhibitor molecule has been spontaneously adsorbed onto the three metal surfaces. Positive values obtained for enthalpy change indicated that the adsorption of inhibitor is endothermic. The data clarified that the inhibition of aluminum and copper in biodiesel blend B20 by TBHQ takes place through physicochemical adsorption mechanism, while in stainless steel occurred by physical adsorption mechanism.

Keywords

Biodiesel, Corrosion, Electrochemical Impedance Spectroscopy, Tert-butylhydroquinone.

1. INTRODUCTION

Biodiesel is currently a very popular renewable eco-friendly energy source which can be produced from vegetable oils, animal fats or algae (Faried et al., 2017). It can be used alone as pure form or it can be used in blend with regular petroleum diesel, in a very conventional way without any need for engine modification and with minimum change of fuel properties (Islam, Taufiq-Yap, & Chan, 2015).

Currently B20 is the most used biodiesel blend (20% biodiesel and 80% petroleum diesel) and it can be used in any diesel engine providing the highest benefits without any mechanical alterations (Deyab, 2016). Despite the environmental advantages of biodiesel and its good properties, the instability of biodiesel can be one of its main drawbacks (Singh, Korstad, & Sharma, 2012).

The auto-oxidation of biodiesel caused by its structure can lead to its corrosive properties, which can be intensified when in contact with metals (Singh, Korstad, & Sharma, 2012). The corrosiveness of biodiesel can be explained by the Nernst equation, which implies that most metals can transfer ions into solutions resulting in abrasion. Different factors such as the mass of the metal, oxidation potential and impurities in the fuel can determine the extent of corrosion (Hoang, Tabatabaei, & Aghbashlo, 2019). Furthermore, the level of metal parts that can dissolve in the fuel can be greater because of the higher lubricity of biodiesel compared to conventional diesel (Singh, Korstad, & Sharma, 2012).

The most common used metals in the manufacturing of diesel engines are aluminum (Al), copper (Cu) and stainless steel (SS). The light weight and high strength of aluminum makes it an essential metal in the automotive industry (Díaz-Ballote, López-Sansores, Maldonado-López, & Garfias-Mesias, 2009). The high thermal and electrical conductivity of copper, as well as its good bearing property also makes it an essential metal in automotive parts such as injectors and fuel pump (Fazal, Haseeb, & Masjuki, 2010). Similarly, pump ring, nozzle and valve bodies in the engine are made of stainless steel due to it high resistance to corrosion and strength (Bahadori, 2014). Hence, the study of corrosion of biodiesel blends and the search for the most effective inhibitor to decrease the corrosiveness of biodiesel and increase the longevity of engine metals is an important aspect to be investigated.

In order to reduce the corrosiveness of biodiesel, it is necessary to reduce its oxidation potential, which can be achieved by a variety of techniques including: low temperature storage, vacuum technology, reducing partial pressure of oxygen in contact, enzyme deactivation, inert gas packaging or the use of antioxidants. Currently, most of these techniques can be expensive and require a lot of energy. With that being said, the use of antioxidants can be the most effective and cost efficient method to inhibit the corrosiveness of biodiesel (Varatharajan & Pushparani, 2018). Organic antioxidant containing oxygen, nitrogen and cyclic compounds are widely used (Bahrami, Hosseini, & Pilvar, 2010).

There is no antioxidant that can be used for all the different types of biodiesel. The effectiveness of the antioxidant primarily depends on the source of feedstock and the degree of unsaturation. Tert-butylhydroquinone (TBHQ) is one antioxidant which can be used for biodiesel made from vegetable oil (Varatharajan & Pushparani, 2018). TBHQ is a phenolic antioxidant soluble in fat, it has oxygen in its structure with an aromatic ring which get adsorbed on the metal surface (Cook & Hackerman, 1951), it is used in the food industry as a preservative for unsaturated oils (Prasad, Siddaramaiah, & Banu, 2015; Varatharajan & Pushparani, 2018). It is also used as an additive in perfumes, resins, varnishes and as an antioxidant in biodiesel. Few studies have been investigated the effect of TBHQ on the inhibition of the corrosiveness of biodiesel. Fernandes et al. (Fernandes, Squissato, Lima, Richter, & Munoz, 2019) investigated the effect of TBHQ antioxidants on the stability and corrosiveness of Moringa oleifera Lam biodiesel upon exposure to different carbon steels (CS1015 and CS4140); they found that TBHQ decreases the oxidation of biodiesel, it also inhibits the corrosion by decreasing the presence of iron in the biodiesel exposed to CS1015. Also, Fernandes et al. (Fernandes et al., 2013) investigated the effect of TBHQ on the corrosion of soybean biodiesel upon exposure to carbon steel and galvanized steel; they found that TBHQ may have acted as a corrosion inhibiter.

Due to the lack of research concerning the use of TBHQ as a corrosion inhibitor of biodiesel blends toward common engine metals, it was important to further investigate the effectiveness of TBHQ and fill the gap within this field of research.

In the present study, TBHQ was investigated as corrosion inhibitor toward aluminum; copper and stainless steel in biodiesel blend B20 using electrochemical impedance spectroscopy method. In addition, the adsorption process and the electrochemical parameters are calculated and discussed.

2. EXPERIMENTAL

2.1 Preparation of pure biodiesel and blend B20

Pure biodiesel samples were prepared by transesterifying corn oil (purchased from a local store) with methanol (purchased from Sigma Aldrich) in the presence of NaOH as a catalyst. The reaction was done at 60°C for 1 hour, then the byproduct glycerol is separated from biodiesel by using a separating funnel (Saba, 2015). The biodiesel is then washed with distilled water to remove all the impurities (Díaz-Ballote et al., 2009).Some of the physicochemical properties of the pure biodiesel are indicated in Table 1. In general, these values are acceptable considering ASTM D6751-20a.

Table 1 The physicochemical properties of the pure biodiesel

Property	Unit	Biodiesel
Appearance	-	Clear, light yellow
Physical State	-	Liquid
Density at 15°C	Kg/m^3	887.7
Flash Point	℃	124
Water content	% vol	0
Kinematic Viscosity	mm^2/s	4.7
Cloud point	°C	-1
Acid number	mg KOH/g	0.18

The petroleum diesel fuel used in this study was purchased from a local station. The biodiesel blend B20 samples used in the present study were prepared by mixing 20% of pure biodiesel and 80% of petroleum diesel.

2.2 Materials and Chemicals

2.2.1 Working electrodes

The working electrodes used in this study were aluminum (Al), copper (Cu) and stainless steel (SS) with chemical composition of each metal (wt %) indicated in Table 2. the chemical composition of all working electrodes was determined using SPECTROMAX arc/spark OES metal analyzer present in TQP Laboratories, Lebanon. The surface of the exposed area of each electrode was 9.15 cm^2. Each electrode was abraded before use with an emery papers from grades 150 - 800, and washed with distilled water, then rinsed with acetone and finally dried before immersion in the blend solution.

Table 2 Chemical analysis of the used aluminum, copper and stainless steel specimens

Element	Mg	C	Si	Mn	P	Na	S	Ni	Cr	Al	Cu	Fe
Al wt.%	0.001	--	0.052	0.011	0.001	0.016	--	0.005	0.004	99.40	--	--
Cu wt. %	0.001	--	0.003	--	--	--	--	0.005	0.001	--	99.80	--
SS wt. %	--	0.045	0.485	1.640	0.001	--	0.003	7.590	19.830	--	--	68.30

2.2.2 Tert- butylhydroquinone (TBHQ)

Tert-butylhydroquinone (TBHQ), (as shown in Fig. 1), was purchased from Sigma Aldrich and used without any further purification.

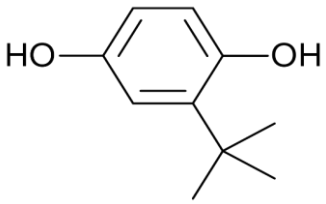

Fig. 1 The molecular structure of TBHQ

2.3 Electrochemical testing

Electrochemical testing was carried out in an electrochemical cell of two-electrode mode; two identical metal working electrode of an exposed area of 9.15 cm^2 (stainless steel (SS), aluminum (Al) or copper (Cu)) of chemical composition in wt% indicated in Table 2; one is connected to auxiliary and reference terminals and the other to the working electrode terminal. The used potentiostat was IVIUM vertex one Technologies with serial No. of V01302; (The frequency range for electrochemical impedance spectroscopy (EIS) measurements was from 0.01 to 9.6 $\times 10^4$ Hz with an applied potential signal amplitude of ± 10 mV around the rest potential). The AC experiment was conducted in the frequency range of 300,000 Hz – 1 Hz at open circuit potential with amplitude of 10 mV peak-to-peak using AC signals. Before the electrochemical measurements, the specimens were immersed in test solution at open circuit potential for 20 minutes to attain a stable state.

3. RESULTS AND DISCUSSION

3.1 Electrochemical impedance spectroscopy (EIS) results

Electrochemical impedance spectroscopy (EIS) is a non-destructive method used to study the electrochemical systems to predict the corrosion rate of the metals. EIS was used to investigate the corrosion inhibition of the TBHQ toward Al, Cu and SS. Fig 2, Fig. 3 and Fig. 4 show the recorded Nyquist plot for the Al, Cu and SS, respectively, in biodiesel blend B20 at various concentrations of TBHQ.

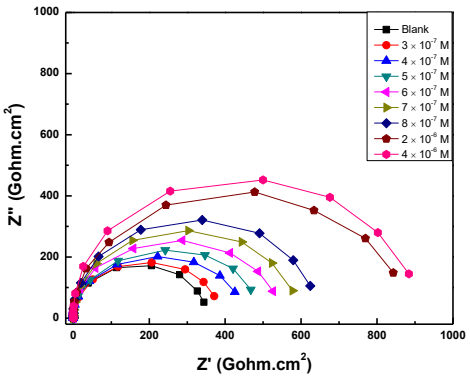

Fig. 2 Nyquist plots for Al in biodiesel blend B20 in the absence and the presence of different concentrations of TBHQ at 30℃

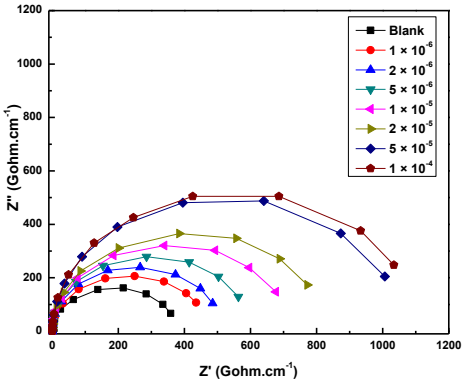

Fig. 3 Nyquist plots for Cu in biodiesel blend B20 in the absence and the presence of different concentrations of TBHQ at 30℃

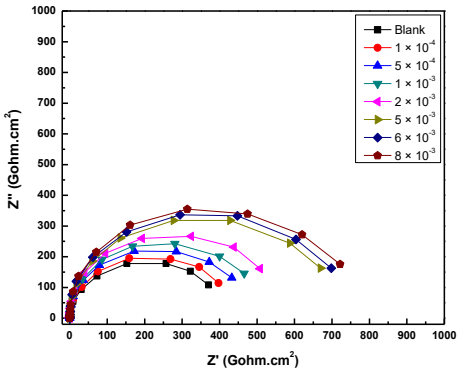

Fig. 4 Nyquist plots for SS in biodiesel blend B20 in the absence and the presence of different concentrations of TBHQ at 30℃

All the impedance response consisted of characteristic depressed semicircle of capacitive type indicating that the dissolution process occurs under activation control. The deviation from a typical semicircle is attributed to inhomogeneity and roughness of the metal surface (Kilo, Rahal, El-Dakdouki, & Abdel-Gaber, 2020). The presence of only one depressed semicircle suggests a single charge transfer process. Addition of TBHQ enlarges the diameter of the semicircle of the Nyquist plots without affecting on the plot shapes. This suggests that the inhibitive action of TBHQ is due to the adsorption of TBHQ molecules on the metal surfaces (Al, Cu and SS) without variation in the corrosion mechanism (Tan, Kassim, & Oo, 2012).

The impedance data of Al, Cu and SS in biodiesel blend B20 are analyzed in terms of equivalent circuit model shown in Fig. 5. It comprises a solution resistance (R_s), charge transfer resistance (R_{ct}) and constant phase element (CPE) (Kilo et al., 2020). The CPE (Qdl,n) is composed of non-ideal double layer capacitance Q_{dl} and a coefficient "n" that quantifies different physical phenomena like surface inhomogeneity, inhibitor adsorption and porous layer formation. The values of EIS parameters obtained from the fitting of the experimental Al, Cu and SS data to the correspondent equivalent circuit are indicated in Tables 3, 4 and 5 respectively.

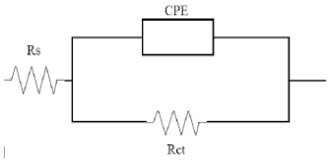

Fig. 5 Schematic for the equivalent circuit model used to fit the impedance data

The corrosion inhibition of TBHQ (% P) was estimated as follows (Umoren, Banera, Alonso-Garcia, Gervasi, & Mirífico, 2013):

$$\% P = [(R_{ct} - R_{cto})]/R_{ct} \times 100 \quad (1)$$

Where R_{cto} and R_{ct}, the charge transfer resistance values (Gohm.cm^2) with and without TBHQ, respectively. The calculated values of %P are indicated in Tables 3, 4 and 5.

The data indicated in Tables 3, 4 and 5 reveals that increasing TBHQ concentration leads to an overall increase in the charge transfer resistance (R_{ct}) that is associated with decrease in non-ideal double layer capacitance Q_{dl} in the biodiesel blend B20. This means that the inhibition efficiency increases with the increase of the concentration of TBHQ, while the corrosion rate decreases with TBHQ concentration. The change in the R_{ct} and Q_{dl} values is due to the gradual replacement of the solution molecules by the organic molecules on the metal surface, decreasing the extent of the metal dissolution. The decrease in Q_{dl} values with concentration is due to the decrease in dielectric constant and/or increase in the thickness of the electrical double layer, suggesting that TBHQ molecules act by adsorption at the metal/solution interface (Deyab, Corrêa, Mazzetto, Dhmees, & Mele, 2019). Inspection of the results also reveals that the inhibition performance of TBHQ increases with increasing concentrations. A maximum inhibition efficiency of about 61.52% for Al was recorded for

THBQ in biodiesel blend B20 at a concentration of $4x10^{-6}$ M, 66.96 % for Cu at a concentration of 1 x 10^{-4} M and 46.36% for SS at a concentration of 8 x 10^{-3} M. The highest value of %P for Al is obtained at $4x10^{-6}$ M concentration which is the lowest concentration used compared to the concentrations of TBHQ used for the other Cu and SS.

Table 3 Electrochemical impedance parameters for the corrosion of Al in biodiesel blend B20 in the absence and the presence of different concentrations of THBQ at 30℃

Conc. ($mol.L^{-1}$)	R_s ($Gohm.cm^2$)	R_{ct} ($Gohm.cm^2$)	n	Q_{dl} ($\mu F.cm^{-2}$)	% P
Blank	0.02	384	1.00	6.25×10^{-11}	---
3×10^{-7}	0.01	428	0.96	6.02×10^{-11}	10.28
4×10^{-7}	0.01	484	0.96	5.85×10^{-11}	20.66
5×10^{-7}	0.02	537	0.98	5.47×10^{-11}	28.49
6×10^{-7}	0.02	588	0.96	4.40×10^{-11}	34.69
7×10^{-7}	0.01	643	0.99	4.28×10^{-11}	40.39
8×10^{-7}	0.02	704	1.00	3.83×10^{-11}	45.28
2×10^{-6}	0.01	952	0.97	2.78×10^{-11}	59.66
4×10^{-6}	0.01	998	0.98	2.67×10^{-11}	61.52

Table 4 Electrochemical impedance parameters for the corrosion of Cu in biodiesel blend B20 in the absence and the presence of different concentrations of THBQ at 30℃

Conc. ($mol.L^{-1}$)	R_s ($Gohm.cm^2$)	R_{ct} ($Gohm.cm^2$)	n	Q_{dl} ($\mu F.cm^{-2}$)	% P
Blank	0.01	413	0.92	5.44×10^{-11}	---
1×10^{-6}	0.02	543	0.88	4.64×10^{-11}	23.94
2×10^{-6}	0.01	580	0.91	4.37×10^{-11}	28.79
5×10^{-6}	0.01	675	0.92	4.27×10^{-11}	38.81
1×10^{-5}	0.02	799	0.92	3.63×10^{-11}	48.31
2×10^{-5}	0.01	911	0.92	3.24×10^{-11}	54.66
5×10^{-5}	0.02	1140	0.97	3.05×10^{-11}	63.77
1×10^{-4}	0.01	1250	0.92	2.62×10^{-11}	66.96

Table 5 Electrochemical impedance parameters for the corrosion of SS in biodiesel blend B20 in the absence and the presence of different concentrations of THBQ at 30℃

Conc. ($mol.L^{-1}$)	R_s ($Gohm.cm^2$)	R_{ct} ($Gohm.cm^2$)	n	Q_{dl} ($\mu F.cm^{-2}$)	% P
Blank	0.01	457	0.92	7.92×10^{-11}	---
1×10^{-4}	0.02	484	0.92	7.60×10^{-11}	5.57
5×10^{-4}	0.01	542	0.92	6.91×10^{-11}	15.68
1×10^{-3}	0.01	580	0.94	6.90×10^{-11}	21.20
2×10^{-3}	0.02	652	0.92	6.02×10^{-11}	29.90
5×10^{-3}	0.02	784	0.95	4.42×10^{-11}	41.70
6×10^{-3}	0.01	816	0.94	4.16×10^{-11}	43.99
8×10^{-3}	0.02	852	0.94	3.89×10^{-11}	46.36

3.2 Adsorption Isotherms

The nature of interactions between Al, Cu and SS surfaces and the TBHQ molecules throughout the corrosion inhibition process can be described by the adsorption isotherms. To discuss the adsorption isotherms, the degree of surface coverage values were obtained from EIS measurements using equation (θ = % P/100).

Fig. 6, Fig. 7 and Fig. 8 show the variation of the degrees of the surface coverage (θ) values with the TBHQ concentration for Al, Cu, SS in biodiesel blend B20 at 30°C. The variation of degree of surface coverage curve is characterized by an initial rising part followed by a constant saturated part at high concentrations.

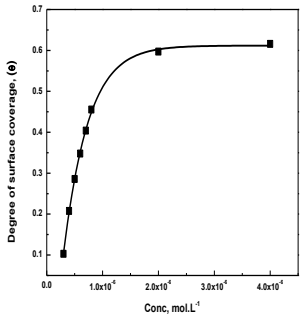

Fig. 6 The variations of degree of surface coverage (θ) of Al with the concentrations of TBHQ in biodiesel blend B20 at 30℃.

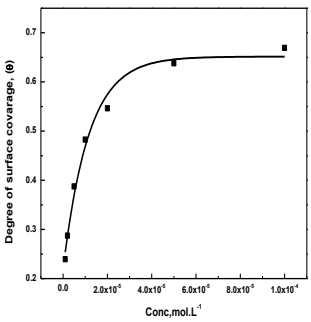

Fig. 7 The variations of degree of surface coverage (θ) of Cu with the concentrations of TBHQ in biodiesel blend B20 at 30℃.

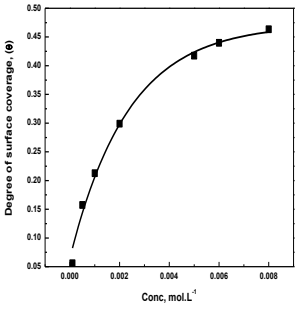

Fig.8 The variations of degree of surface coverage (θ) of SS with the concentrations of TBHQ in biodiesel blend B20 at 30℃.

Attempts were made to fit (θ) values to different isotherms including Langmuir, Freundlich, Kinetic-Thermodynamic model and Flory-Huggins (Temkin, 1941) according to the following equations:

Langmuir Isotherm: $\theta/1-\theta = K_{ads}[C]$ (2)

Freundlich isotherm: $\log \theta = \log K_{ads} + (1/n)\log C$ (3)

Kinetic-Thermodynamic Isotherm: $\log [\theta/ (1- \theta)] = \log K' + y \log C_{inh}$; $K_{ads} = K'^{1/y}$ (4)

Flory-Huggins Isotherm: $\log (\theta/C) = \log xK + x \log(1-\theta)$, (5)

Where "C" is the inhibitor concentration, "θ" is the coverage degree, n is an empirical constant, "y" is the number of adsorbed molecules in an active site, "x" is the size parameter and is a measure of the number of adsorbed solvent molecules substituted by a given inhibitor molecule and "K" is the adsorption equilibrium constant.

The Langmuir theory assumes that the adsorption occurs at specific homogenous sites, sites with equivalent energy for the adsorbed molecules, where the adsorption occurs in a monolayer on the surface of the adsorbent and each site being responsible for the adsorption of only a single molecule. The plot of (θ/1-θ) vs. C shown in Fig. 9, Fig. 10 and Fig. 11 gives a straight line with an intercept of -0.31, 0.26, 0.07 for Al, Cu, and SS respectively which confirms that the adsorption of TBHQ on these metals does not obey Langmuir adsorption isotherm indicating non ideal behavior.

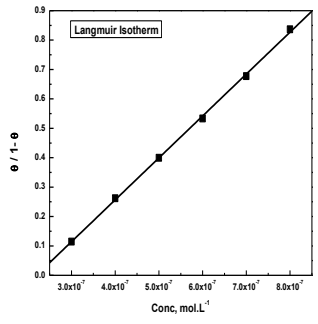

Fig. 9 Langmuir adsorption isotherm for Al in biodiesel blend B20 containing TBHQ at 30℃.

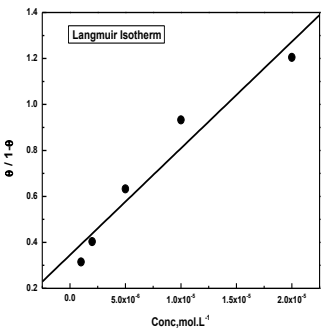

Fig. 10 Langmuir adsorption isotherm for Cu in biodiesel blend B20 containing TBHQ at 30℃.

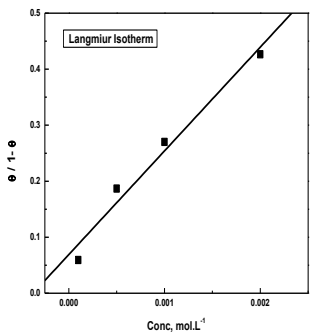

Fig. 11 Langmuir adsorption isotherm for SS in biodiesel blend B20 containing TBHQ at 30℃.

The Freundlich isotherm states the quantitative relationship of the inhibiting compound and the molecular concentration of inhibitor molecules absorbed onto the metals which varies at specific concentrations according to equation 3 (Foad El-Sherbini, Abdel Wahaab & Deyab, 2005). The value of (1/n) is used to describe the ease of adsorption. Usually, when $0 < (1/n) < 1$, the adsorption is

believed to be easy, and moderate or difficult when (1/n) =1 or (1/n) > 1 respectively (OZa & Sinha, 1982). On the other hand, the Kinetic-thermodynamic isotherm considers that active sites can be occupied by more than one inhibitor molecule or that a single inhibitor molecule can adsorb in more than one active site (parameter y). y < 1 shows that a single molecule involved in the adsorption process has been adsorbed on more than one active site, i.e., y is the number of inhibitory molecules occupying an active site on the metal surface (Madkour & Elroby, 2015).

Fig. 12, 13 and 14 show the Freundlich, Kinetic-Thermodynamic and Florry-Huggins adsorption isotherm models considered in this study. The R^2 values for each isotherm model indicated in Table 6 were used to determine the suitable model. The data shows that the adsorption of the inhibitor TBHQ follows Freundlich and Kinetic-Thermodynamic model on the three metal surfaces (Al, Cu, SS) in biodiesel blend B20 at 30℃.

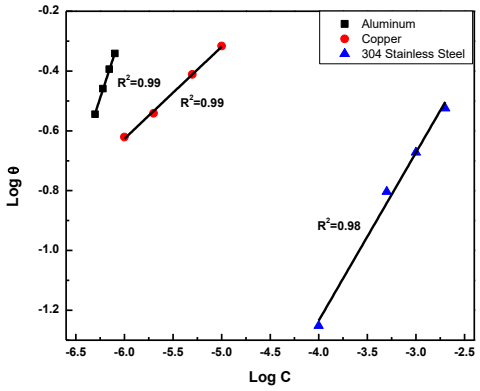

Fig. 12 Freundlich adsorption isotherm for Al, Cu and SS in B20 containing TBHQ at 30℃.

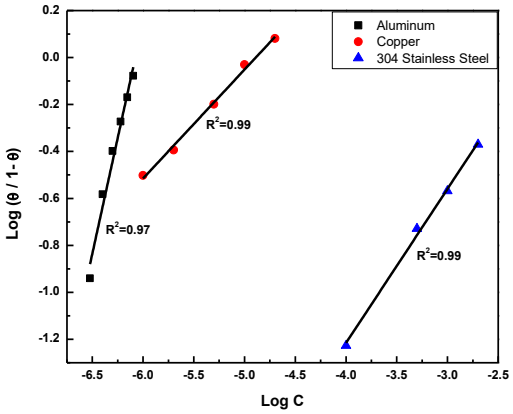

Fig. 13 Kinetic-Thermodynamic model for Al, Cu and SS in B20 containing TBHQ at 30℃.

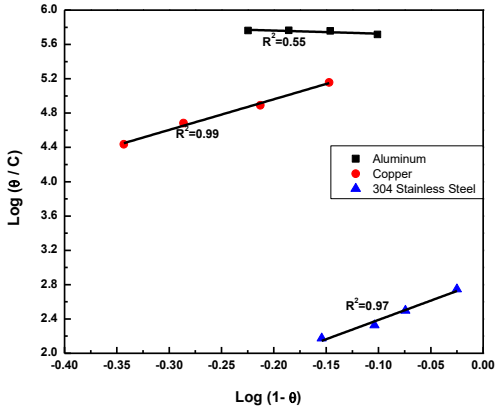

Fig. 14 Flory-Huggins model for Al, Cu and SS in B20 blend containing TBHQ at 30℃.

Table 6 R^2 values for the various adsorption isotherms considered

Metal	Freundlich model R^2	Kinetic-Thermodynamic model R^2	Flory-Huggins R^2
Al	0.99	0.97	0.55
Cu	0.99	0.99	0.99
SS	0.98	0.99	0.97

The parameters obtained from Freundlich and Kinetic-Thermodynamic model are indicated in Table 7.

Table 7 Linear fitting adsorption parameters for Al, Cu and SS in biodiesel blend B20 containing TBHQ at 30℃ according to Freundlich and Kinetic-Thermodynamic models

Inhibitor	Metal	Freundlich Model		Kinetic-Thermodynamic Model		
		K	1/n	K	y	1/y
TBHQ	Al	527910	0.994	1191106.3	1.97	0.51
TBHQ	Cu	16.52	0.307	77538.2	0.46	2.16
TBHQ	SS	10.28	0.562	140.46	0.66	1.52

The Kinetic-Thermodynamic plot can be used to determine the associated parameters such as the reciprocal of y which is used to describe the number of active sites on the surface occupied by one molecule of the inhibitor. In case of Al, the number of the active sites occupied by a single inhibitor (1/y) is less than one, indicating the adsorption of small molecules of TBHQ. However, (1/y) obtained for Cu and SS are greater than unity indicating that bulky molecules of TBHQ are adsorbed on more than one active sites on the Cu and SS metal surface.

Furthermore, it is well known that the inhibition efficiency is basically a function of the magnitude of inhibitor's binding constant K, which designates the strength between adsorbate and adsorbent, in which large values of K mean better and stronger interaction, whereas small values of K mean that the interaction between the inhibitor molecules and the metal surface is weak (Abd-El-Nabey, Abdel-Gaber, Elawady, & El-Housseiny, 2012). As indicated in Table 7, the adsorption equilibrium constants, K_{ads} are positive, indicating the feasibility of the adsorption of the inhibitor to the metal surface. According to the numerical values of K obtained from the Kinetic-Thermodynamic model, it was found that the magnitude of inhibitor's binding constant K_{ads} in Al was higher than K_{ads} in Cu and SS. This suggests a stronger interaction between the Al metal surface and the small inhibitor molecules compared to those formed between the bulky molecules and Cu and SS surface. This explains the improved inhibition efficiency of TBHQ with aluminum compared to copper and SS. Similar observation was observed according the numerical values of K obtained from Frerundlich model.

The binding constants of the kinetic-thermodynamic model were used to calculate the Gibbs free energy of adsorption (ΔG_{ads}), as indicated in Table 8, according to the following equation (Morales-Gil, Negrón-Silva, Romero-Romo, Ángeles-Chávez, & Palomar-Pardavé, 2004; Palomar-Pardavé et al., 2012):

$$\Delta G^{\circ}_{ads} = - RT \ln (K_{ads}) \quad (6)$$

Where R is the molar gas constant, T is the absolute temperature in Kelvin, K_{ads} is the adsorption equilibrium constant obtained from the isotherm.

Table 8 ΔG°_{ads} value of TBHQ in biodiesel blend B20 for Al, Cu and SS

Inhibitor	Metal	ΔG°_{ads} ($kJ.mol^{-1}$)
TBHQ	Al	-35.24
TBHQ	Cu	-28.36
TBHQ	SS	-12.46

As indicated in Table 8, the negative values of ΔG°_{ads} obtained indicate a spontaneous adsorption of TBHQ on the three used metal surfaces and reflects the stability of the adsorbed layers on the metals. In addition, it is well-known that the values of ΔG°_{ads} of the order of - 20 kJ mol/1 are consistent with the electrostatic interactions between the charged molecules and the metal (physisorption), while those around - 40 kJ moL/l or more negative are associated with chemisorption as a result of sharing or transfer of electron pair or p electrons from organic molecules to the metal surface to form a coordinate type of bond (chemisorption) (Ashassi-Sorkhabi, Shabani, Aligholipour, & Seifzadeh, 2006; Eddy & Ebenso, 2008; Nwabanne & Okafor, 2012). It was clearly observed that the adsorption using aluminum and copper metals is not merely physisorption or chemisorption but obey a comprehensive adsorption mechanism (physicochemical adsorption), however using SS, the absolute values of ΔG°_{ads} indicates that the corrosion inhibition takes action due to electrostatic interactions between charged molecules and charged metal (physical adsorption).

3.3 Effect of temperature

The effect of temperature on the performance of TBHQ as corrosion inhibitor is investigated by EIS measurements in the temperature range 303-333 K. Fig. 15(a) and (b) shows the Nyquist plots obtained for Cu in B20 in the absence and the presence of TBHQ at different temperatures. It indicates that, as the temperature increases the size of the depressed semicircles decreases, which indicates a decrease in the charge transfer resistance (R_{ct}) values. Similar behavior was observed for Al and SS in biodiesel blend B20.

This indicates that the corrosion rate increases with the increase in temperature both in uninhibited and inhibited solutions. The decrease in the inhibition efficiency can be attributed to increases rate of dissolution process of metal and partial desorption of the inhibitor from the metal surface with an increase in temperature (Schorr & Yahalom, 1972).

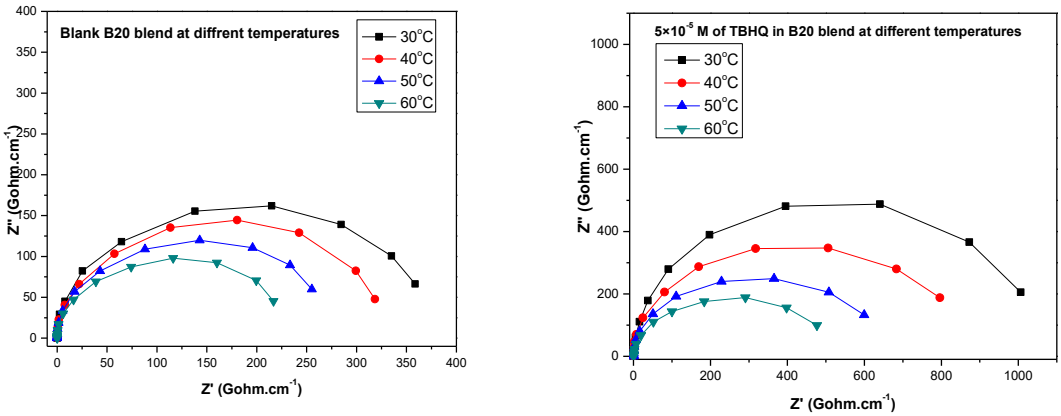

(a) (b)

Fig. 15 Nyquist impedance plots for Cu in biodiesel blend B20 in (a) the absence and (b) the presence of $5x10^{-5}$ M of TBHQ at different temperatures

3.4 Activation and thermodynamic parameters

The activation and thermodynamic parameters are of great importance for elucidating the mechanism of corrosion inhibition of the three metals. The activation and thermodynamic parameters for Al, Cu and SS corrosion in biodiesel blend B20 in the absence and presence of different concentrations TBHQ were obtained by applying Arrhenius type plot (Eq. 7) and transition state (Eq. 8) (Umoren et al., 2013):

$$\text{Ln } \upsilon = \text{Ln } A - (E_a/RT) \quad (7)$$

Where υ is the corrosion rate, E_a is apparent activation energy, A; the pre-exponential factor, and R is the universal gas constant.

$$\upsilon = RT/Nh\, e^{\Delta S^*/R} \cdot e^{-\Delta H^*/RT} \quad (8)$$

Where ΔH* is the apparent enthalpy of activation, ΔS* is the apparent entropy of activation, h is the Planck's constant and N is the Avogadro's number and T the thermodynamic temperature.

A plot of ln (υ) versus (1/T) gave a straight line as shown in Fig. 16 with a slope of –Ea for three metals used. The values of activation energy are indicated in Table 9. By comparing the apparent activation energy (E_a) values, several information about the mechanism of inhibiting action was obtained. The data show that the activation energy of Al, Cu and SS in biodiesel blend B20 in the presence of TBHQ is higher than in the blank solutions (biodiesel blend B20). This increase in inhibited biodiesel blend B20 suggests a protective effect of TBHQ molecules of the three metal surfaces. It can also be seen that the activation energy of Cu is higher than that of Al and SS reflecting high protection efficiency in case of Cu compared to the other two metals.

A plot of Ln (υ/T) versus (1/T) gave a straight line as shown in Fig. 17 with a slope of (-ΔH*/R) and intercept of (Ln R/Nh + ΔS*/R). From the slope and intercept, ΔH* and ΔS* were calculated and indicated in Table 9. The positive sign of enthalpies ΔH* reflect the endothermic nature of the metals dissolution process (Mu, Li, & Li, 2004). Moreover, the presence of the inhibitor

produces higher value of ΔH* than those obtained for the uninhibited solutions. This suggests that metal dissolution in biodiesel blend B20 requires more energy in the presence of the inhibitor TBHQ. Higher values of ΔH* using copper metal means that the dissolution of copper in biodiesel blend B20 in the presence of TBHQ is difficult compared to the other two metals.

In addition, the negative and large values of the entropy of activation, ΔS*, implies that the activation complex represents an association rather than a dissolution step meaning that a decrease in a disordering takes place on going from reactants to activated complex (Deyab, 2015).

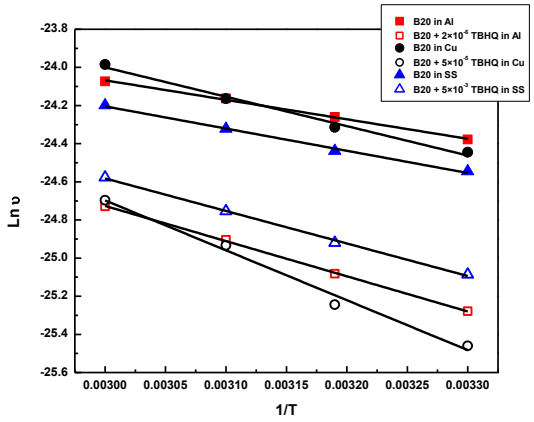

Fig. 16 Variation of ln υ with 1/T of Al, Cu and SS in biodiesel blend B20 in the absence and the presence of TBHQ.

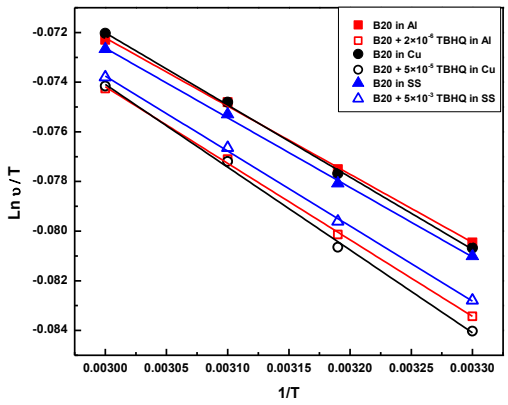

Fig. 17 Variation of ln (υ /T) with 1/T of Al, Cu and SS in biodiesel blend B20 in the absence and the presence of TBHQ.

Table 9 Activation parameters of the dissolution of Al, Cu and SS in biodiesel blend B20 in the absence and presence of TBHQ

Metal	Inhibitor	E_a (kJ.mol^{-1})	ΔH* (J.mol^{-1})	ΔS* (J.mol^{-1}.K^{-1})
Al	Blank	8.50	228.38	-197.455
	TBHQ	15.34	256.39	-197.387
Cu	Blank	12.81	241.79	-197.407
	TBHQ	21.75	277.34	-197.324
SS	Blank	9.69	233.26	-197.444
	TBHQ	14.19	251.24	-197.399

4. CONCLUSION

Tert-butylhydroquinone (TBHQ) was found to be an effective inhibitor for the Al, Cu and SS corrosion in biodiesel blend B20 at 30℃. It was observed that the inhibition efficiency increases with increasing the concentration of TBHQ and the maximum efficiency was observed at $4x10^{-6}$ M concentration using aluminum metal. Double layer capacitances decreases by adding TBHQ into biodiesel blend B20, indicating the adsorption of TBHQ on Al, Cu and SS surfaces. This adsorption obeys Freundlich and Kinetic-Thermodynamic models and a higher value of K_{ads} for Al obtained suggests a strong interaction between TBHQ and Al surface compared to the other two metals. Moreover, $\Delta G°_{ads}$ values indicate a strong and spontaneous adsorption of the TBHQ on the three metal surfaces.

REFERENCES

Abd-El-Nabey, B. A., Abdel-Gaber, A. M., Elawady, G. Y., & El-Housseiny, S. (2012). Inhibitive Action of Some Plant Extracts on the Alkaline Corrosion of Aluminum. *International journal of electrochemical science*, *7*, 7823.

Ashassi-Sorkhabi, H., Shabani, B., Aligholipour, B., & Seifzadeh, D. (2006). The effect of some Schiff bases on the corrosion of aluminum in hydrochloric acid solution. *Applied Surface Science*, *252*(12), 4039-4047. doi:10.1016/j.apsusc.2005.02.148

Bahadori, A. (2014). Corrosion and materials selection : a guide for chemical and petroleum industries.

Bahrami, M. J., Hosseini, S. M. A., & Pilvar, P. (2010). Experimental and theoretical investigation of organic compounds as inhibitors for mild steel corrosion in sulfuric acid medium. *Corrosion Science*, *52*(9), 2793-2803. doi:10.1016/j.corsci.2010.04.024

Cook, E. L., & Hackerman, N. (1951). Adsorption of Polar Organic Compounds on Steel. *The Journal of Physical Chemistry*, *55*(4), 549-557. doi:10.1021/j150487a010

Deyab, M. A. (2015). Egyptian licorice extract as a green corrosion inhibitor for copper in hydrochloric acid solution. *Journal of Industrial and Engineering Chemistry*, *22*, 384-389. doi:https://doi.org/10.1016/j.jiec.2014.07.036

Deyab, M. A. (2016). The inhibition activity of butylated hydroxytoluene towards corrosion of carbon steel in biodiesel blend B20. *Journal of the Taiwan Institute of Chemical Engineers*, *60*, 369-375. doi:https://doi.org/10.1016/j.jtice.2015.10.035

Deyab, M. A., Corrêa, R. G. C., Mazzetto, S. E., Dhmees, A. S., & Mele, G. (2019). Improving the sustainability of biodiesel by controlling the corrosive effects of soybean biodiesel on aluminum alloy 5052 H32 via cardanol. *Industrial Crops and Products*, *130*, 146-150. doi:10.1016/j.indcrop.2018.12.053

Díaz-Ballote, L., López-Sansores, J. F., Maldonado-López, L., & Garfias-Mesias, L. F. (2009). Corrosion behavior of aluminum exposed to a biodiesel. *Electrochemistry Communications*, *11*(1), 41-44. doi:10.1016/j.elecom.2008.10.027

Eddy, N., & Ebenso, E. (2008). Adsorption and inhibitive properties of ethanol extracts of Musa sapientum peels as a green corrosion inhibitor for mild steel in H2SO4. *African Journal of Pure and Applied Chemistry*, *2*(6), 46-54.

Faried, M., Samer, M., Abdelsalam, E., Yousef, R. S., Attia, Y. A., & Ali, A. S. (2017). Biodiesel production from microalgae: Processes, technologies and recent advancements. *Renewable and Sustainable Energy Reviews*, *79*, 893-913. doi:10.1016/j.rser.2017.05.199

Fazal, M. A., Haseeb, A. S. M. A., & Masjuki, H. H. (2010). Comparative corrosive characteristics of petroleum diesel and palm biodiesel for automotive materials. *Fuel Processing Technology*, *91*(10), 1308-1315. doi:10.1016/j.fuproc.2010.04.016

Fazal, M. A., Suhaila, N. R., Haseeb, A. S. M. A., Rubaiee, S., & Al-Zahrani, A. (2018). Influence of copper on the instability and corrosiveness of palm biodiesel and its blends: An assessment on biodiesel sustainability. *Journal of Cleaner Production*, *171*, 1407-1414. doi:10.1016/j.jclepro.2017.10.144

Fernandes, D. M., Montes, R. H. O., Almeida, E. S., Nascimento, A. N., Oliveira, P. V., Richter, E. M., & Muñoz, R. A. A. (2013). Storage stability and corrosive character of stabilised biodiesel exposed to carbon and galvanised steels. *Fuel*, *107*, 609-614. doi:10.1016/j.fuel.2012.11.010

Fernandes, D. M., Squissato, A. L., Lima, A. F., Richter, E. M., & Munoz, R. A. A. (2019). Corrosive character of Moringa oleifera Lam biodiesel exposed to carbon steel under simulated storage conditions. *Renewable Energy*, *139*, 1263-1271. doi:10.1016/j.renene.2019.03.034

Foad El-Sherbini, E.E.; Abdel Wahaab, S.M.; Deyab, M. Ethoxylated fatty acids as inhibitors for the corrosion of zinc in acid media. Mats. Chem. & Phys. 2005, 89(2-3), 183-191. DOI: http://dx.doi.org/10.1016/j.matchemphys.2003.09.055

Hoang, A. T., Tabatabaei, M., & Aghbashlo, M. (2019). A review of the effect of biodiesel on the corrosion behavior of metals/alloys in diesel engines. *Energy Sources, Part A: Recovery, Utilization, and Environmental Effects*, *42*(23), 2923-2943. doi:10.1080/15567036.2019.1623346

Islam, A., Taufiq-Yap, Y. H., & Chan, E.-S. (2015). Advanced technologies in biodiesel : introduction to principles and emerging trends.

Kilo, M., Rahal, H. T., El-Dakdouki, M. H., & Abdel-Gaber, A. M. (2020). Study of the corrosion and inhibition mechanism for carbon steel and zinc alloys by an eco-friendly inhibitor in acidic solution. *Chemical Engineering Communications*, 1-10. doi:10.1080/00986445.2020.1811239

Madkour, L. H., & Elroby, S. K. (2015). Inhibitive properties, thermodynamic, kinetics and quantum chemical calculations of polydentate Schiff base compounds as corrosion inhibitors for iron in acidic and alkaline media. *International Journal of Industrial Chemistry, 6*(3), 165-184. doi:10.1007/s40090-015-0039-7

Morales-Gil, P., Negrón-Silva, G., Romero-Romo, M., Ángeles-Chávez, C., & Palomar-Pardavé, M. (2004). Corrosion inhibition of pipeline steel grade API 5L X52 immersed in a 1 M H2SO4 aqueous solution using heterocyclic organic molecules. *Electrochimica Acta, 49*(26), 4733-4741. doi:10.1016/j.electacta.2004.05.029

Mu, G., Li, X., & Li, F. (2004). Synergistic inhibition between o-phenanthroline and chloride ion on cold rolled steel corrosion in phosphoric acid. *Materials Chemistry and Physics, 86*, 59–68. doi:10.1016/j.matchemphys.2004.01.041

Nwabanne, J., & Okafor, V. (2012). Adsorption and Thermodynamics Study of the Inhibition of Corrosion of Mild Steel in H2SO4 Medium Using Vernonia amygdalina. *Journal of Minerals and Materials Characterization and Engineering, 11*, 885-890.

OZa BN, Sinha RS. Thermodynamic study of corrosion behaviour of high strength Al-Mg alloy in phosphoric acid in presence of halides. Tanstact. saest. 1982;17/4:281-285.

Palomar-Pardavé, M., Romero-Romo, M., Herrera-Hernández, H., Abreu-Quijano, M. A., Likhanova, N. V., Uruchurtu, J., & Juárez-García, J. M. (2012). Influence of the alkyl chain length of 2 amino 5 alkyl 1,3,4 thiadiazole compounds on the corrosion inhibition of steel immersed in sulfuric acid solutions. *Corrosion Science, 54*, 231-243. doi:10.1016/j.corsci.2011.09.020

Prasad, N., Siddaramaiah, B., & Banu, M. (2015). Effect of antioxidant tertiary butyl hydroquinone on the thermal and oxidative stability of sesame oil (sesamum indicum) by ultrasonic studies. *J Food Sci Technol, 52*(4), 2238-2246. doi:10.1007/s13197-014-1276-z

Saba, T. (2015). *Biodiesel production from refined sunflower vegetable oil over zeolite supported catalysts.* (Master's), University of Balamand.

Schorr, M., & Yahalom, J. (1972). The significance of the energy of activation for the dissolution reaction of metal in acids. *Corrosion Science, 12*, 867-868.

Singh, B., Korstad, J., & Sharma, Y. C. (2012). A critical review on corrosion of compression ignition (CI) engine parts by biodiesel and biodiesel blends and its inhibition. *Renewable and Sustainable Energy Reviews, 16*(5), 3401-3408. doi:10.1016/j.rser.2012.02.042

Tan, K. W., Kassim, M. J., & Oo, C. W. (2012). Possible improvement of catechin as corrosion inhibitor in acidic medium. *Corrosion Science, 65*, 152-162. doi:10.1016/j.corsci.2012.08.012

Temkin, M. I. (1941). Adsorption Equilibrium and the Kinetics of Processes on Nonhomogeneous Surfaces and in the Interaction between Adsorbed Molecules. *Zhurnal Fiziche- skoi Khimii, 15*, 296-332.

Umoren, S. A., Banera, M. J., Alonso-Garcia, T., Gervasi, C. A., & Mirífico, M. V. (2013). Inhibition of mild steel corrosion in HCl solution using chitosan. *Cellulose, 20*(5), 2529-2545. doi:10.1007/s10570-013-0021-5

Varatharajan, K., & Pushparani, D. S. (2018). Screening of antioxidant additives for biodiesel fuels. *Renewable and Sustainable Energy Reviews, 82*, 2017-2028. doi:10.1016/j.rser.2017.07.020